Stacked Coupled-Disk MEMS Resonators for RF Applications

Knut H. Nygaard[1], Christopher Grinde[2], Tor A. Fjeldly[3]

[1]Dept. of Engineering, Oslo University College, Oslo, Norway
[2]Dept. of Engineering, Vestfold University College, Horten, Norway
[3]Dept. of Electronics and Telecommunication, Norwegian University of Science and Technology, UniK – University graduate Center, Kjeller Norway

ABSTRACT

We present a novel, stacked coupled-disk resonator where the silicon discs vibrate in radial contour modes, actuated by electrodes wrapped around the disk periphery. The self-aligned, central stem mediates the coupling and also anchors the stack to the substrate. Operating near-identical discs in the fundamental mode, their acoustic nodes are located at the center, and the coupling strength is determined by the stem diameter. Hence, the stem radius determines the resulting splitting of the resonance. Here, we consider double-disk devices with a radius of 36 μm operating near 150 MHz. The fabrication process for the present resonator is discussed.

Keywords: MEMS resonator, coupled resonators, RF.

1 INTRODUCTION

RF MEMS resonators are of considerable interest for applications in numerous electronic systems, including filters, oscillators, mixers, channel selectors, etc., in areas such as signal processing and transmission [1]. Properties such as high *Q*, low power consumption, and prospects of on-chip integration pave the way for new, high-performance system architectures. It is, for example, possible to use a MEMS switchable channel bank in a transceiver, making significant power saving possible in addition to further size reduction. Further reduction in power consumption may be achieved by making use of a switchable MEMS resonator oscillator in combination with a micromechanical mixer-filter such as an RF channel selector. This approach may be refined by using a single MEMS resonator oscillator in combination with a micromechanical mixer-filter as an IF channel selector.

In the transmitter section of a transceiver, it is also possible to use the switchable MEMS resonator oscillator in combination with a MEMS RF channel selector before the antenna. MEMS filter banks may also be used as a part of a signal processing scheme by dividing up a given bandwidth into a number of subbands, where each is subject to subsampling. This reduces the bandwidth requirement before an optional AD conversion. Such an implementation saves both space and power.

For RF operation, miniaturized polysilicon disk resonators can be fabricated with resonance frequencies up the GHz range [1]. In particular, circular disk resonators operating in radial contour modes have been shown to combine RF operation with *Q* factors in the thousands, greatly outperforming comparable transistor implementations. The resonator is actuated by electrodes wrapped around the disk periphery. The self-aligned, central stem anchors the disk to the substrate. The high *Q* comes from the near-negligible damping from air, thermo-elastic effect, and surface effects. The dominant loss mechanism is instead losses through the stem and into the substrate [2,3]. But even this loss is quite limited since the stem sits at the central acoustic node of the disk. Even this loss may be further reduced by replacing the polysilicon disk with one made from polydiamond, which enhances the acoustic mismatch between the disk and the stem.

2 COUPLED DISK RESONATOR

Here, we propose a novel, stacked coupled-disk resonator where two identical silicon discs are attached to the same stem, as indicated schematically in Fig. 1. The stem mediates the mechanical coupling between the disks, resulting in a splitting of the resonances into a symmetric and an anti-symmetric mode. Because of the acoustic node at the center of the disks, the coupling strength, and therefore, also the mode splitting, will depend on the stem diameter. Hence, a slender stem will bring the modes closer together to give a band-pass filter characteristic, and a wider stem gives well-separated modes where the resonator may be operated as an oscillator at either of the two frequencies.

2.1 Equivalent circuit

The coupled resonator may be described in terms a simplified electric lumped-element equivalent circuit corresponding to that of a 3rd order band-pass filter, see Fig. 2. Here, the coupling is modeled by a shunt capacitor, while the two (nearly-identical) single resonators are shown as series LCR sub-circuits in the top branches of the equivalent circuit. Their elements L_R, C_R, and R_R are derived straightforwardly from the mechanical properties

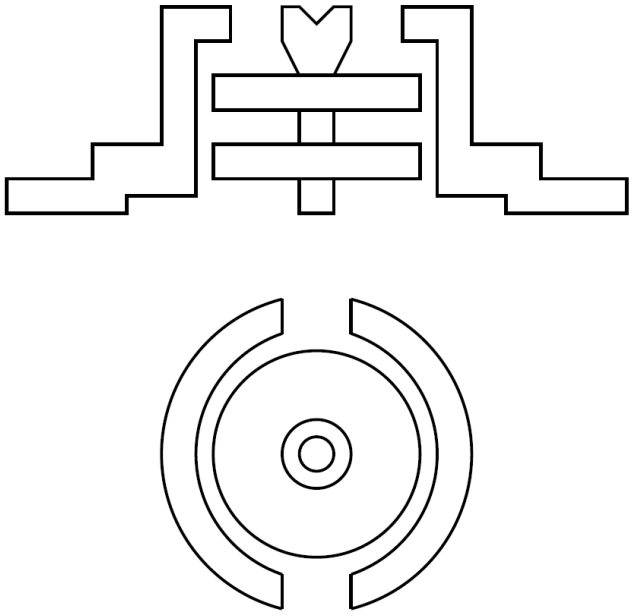

Figure 1: Schematic vertical (top) and horizontal (bottom) cross-sectional views of the proposed double disk resonator.

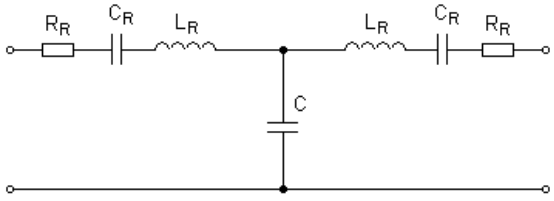

Figure 2: Equivalent circuit of the coupled double disk resonator consisting of the two single-resonator LRC equivalents on top and the coupling network in the middle.

of the resonators [1]. The series motional resistance R_R reflects the loss via the stem to the substrate, and is proportional to $1/Q$ [1]. The single-resonator parameter values are given by

$$L_R = \frac{m_{re}}{\eta_1\eta_2}; \quad C_R = \frac{\eta_1\eta_2}{k_{re}}; \quad R_R = \frac{c_{re}}{\eta_1\eta_2} = \frac{\sqrt{m_{re}k_{re}}}{Q\eta_1\eta_2} \qquad (4)$$

where m_{re}, k_{re} are the equivalent disk mass at the disk perimeter, the equivalent stiffness, and the equivalent electromechanical coupling between the electrodes and the disk, respectively. η_1 and η_2 are the electromechanical coupling factors related to the two ports.

The loss mechanism can be analyzed mechanically by considering separately the disks, the stem sections, and the substrate, and subsequently by connecting them in a self-consistent manner [3]. The vertical vibration of the disk centers propagate throughout the double disk assembly. A part of the associated vibrational energy acts to couple the two disks though the upper stem, giving rise to the coupling capacitor C in equivalent circuit of Fig. 2. Some of energy is transferred to a anchor point where it causes an oscillating deformation of the substrate. We note that the substrate deforms easily because of the relatively low stiffness of the 2 μm SiO_2 layer on top of the silicon substrate (see below). The deformation in the lower stem is small compared to this and can be neglected to lowest order.

The ratio between the reactance of the shunt capacitor C and that of the single-resonator reactance determines the pass-band ripple in the filter. A weak coupling (small C) gives a small mode separation and little ripple. Optimal pass-band filter characteristics are ideally obtained when the total resistance $R_R + R_G$ on the generator (input) side and $R_R + R_L$ on the load (output) side satisfy the requirements for standard filter types such as, for example, Butterworth or Chebyshev filters. However, owing to mechanical constraints, such as the large values of R_R in practical realizations, it may be difficult to achieve ideal filter characteristics, except when the separation between the two vibrational modes is quite small.

Here, we specifically consider a double-disk device with disk diameter of 36 μm, disk thickness of 1.8 μm, stem diameter of 2 μm, and disk-to-electrode gap of 87 nm. The single resonators operate in a fundamental mode near 150 MHz, corresponding well to the LC-product obtained from (4).

Comparisons between simulations based on the presents equivalent circuit, adjusted for a small asymmetry in resonator values, and physical simulations using COMSOL Multiphysics, show that the value of C is about $2\text{x}10^{-15}$ F. This gives a mode separation of 41 kHz, as indicated in Fig. 3. From the same comparison we find a Q of about 8000.

In practice, a still lower value of Q (and a higher value of R_R can be expected. This tends to flatten the response between the peaks, to give better pass-band characteristics. A example of a simulation for this case based on the equivalent circuit is shown in Fig. 4.

3 FABRICATION

The process to fabricate a stacked double-disk structure is an extension of that given in [1]. The cross section with the various layers of the device prior to release etch is shown in Fig.3. Starting with a 100 mm Okmetic, <100> n-type 1-5 Ohm cm wafers, the first step is to make a ground plane using $PoCl_3$ doping. This layer is separated from the active components by a thermal oxide about 2μm thick and a layer of 350 nm silicon nitride. Holes through the nitride and oxide for connecting to the ground plane are etched using a combination of wet and dry etches. A 350 nm layer of polysilicon for inter-connects, is deposited, $PoCl_3$ doped, and patterned.

To form the disk structures and the spacers between, three alternating layers of 0.8 μm PVD oxide and two layers of polysilicon are deposited. The polysilicon layers

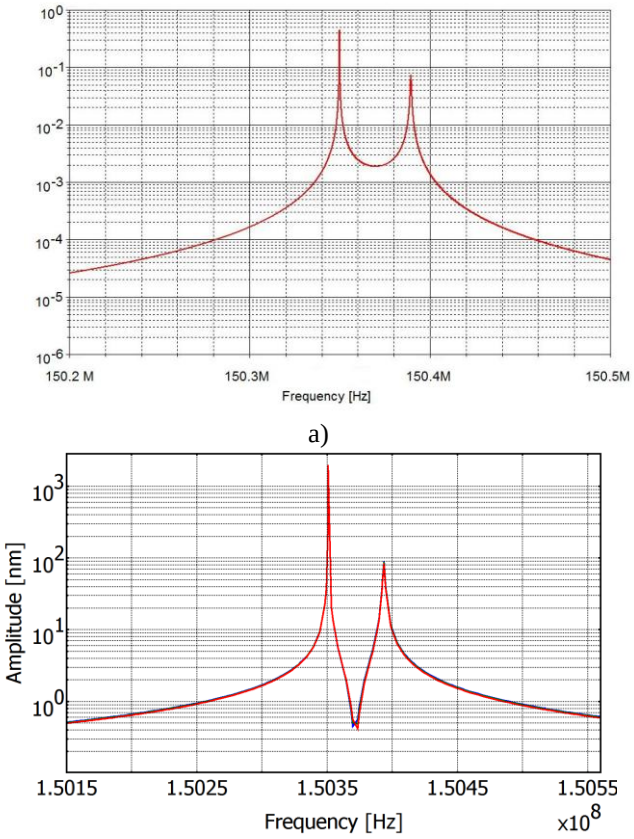

Figure 3: Modeled (a) and simulated (COMSOL) (b) transfer characteristics of the coupled double-disk resonator with disk diameters of 36 μm and stem diameter of 2 μm.

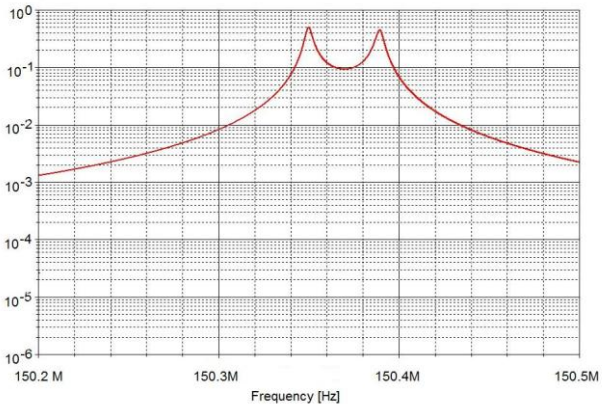

Figure 4: Modeled transfer characteristics of the coupled double-disk resonator with a reduced value of *Q*.

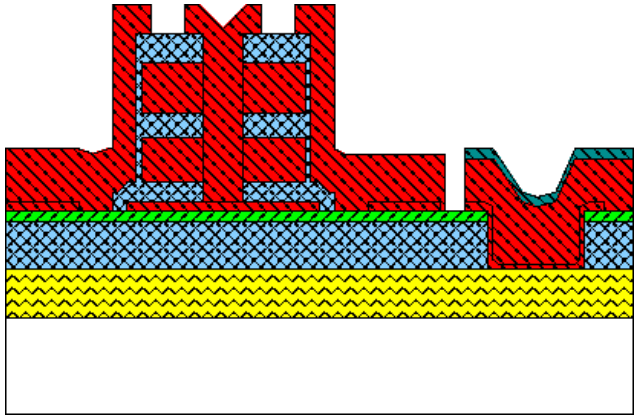

Figure 4: Idealized cross section if the device prior to etching the sacrificial oxide.

are deposited in two 0.75 μm layers with an intermediate $PoCl_3$ diffusion doping step. A sequence of DRIE steps terminating towards the bottom layer of sacrificial oxide is then employed to form the circular disks and the centre hole for the stem.

To form the 100 nm electrode gap, a thermal oxide is grown. In order to remove the oxide in the centre hole, this oxide is patterned and etched with a isotropic dry etch using a negative resist. This is necessary because it would be difficult to expose resist at the bottom of the small diameter centre hole.

A 0.8 μm layer of polysilicon is then deposited in two steps with an intermediate $PoCl_3$ doping to form the electrodes and stem before a thin layer of aluminum for the bonding pads is sputtered and patterned. Using DRIE the last polysilicon layer is etched. Finally, all exposed oxide is etched using HF-vapor phase etching. Processing of devices is in progress at the SINTEF, MinaLAB.

ACKOWLEDGEMENTS

This work was supported by the Norwegian Research Council under contract No. 159559/130 (SMIDA).

REFERENCES

[1] J. Wang, Z. Ren, C.T.-C. Nguyen, IEEE Trans. Ultrason., Ferroelect. and Freq. Contr., vol 51, pp. 1607-1628, 2004.

[2] D. S. Bindel and S. Govindjee, Int. J. Numer. Meth. Engng, vol. 64, pp. 789-818, 2005. 18th IEEE Int. Conf. Micro Electro Mechanical Syst., 2005, pp. 133-136.

[3] Z. Hao and F. Ayazi, Sensors and Actuators A, Vol 134, pp. 582-593, 2007.